Polymer Journal, Vol. 39, No. 10, pp. 1047–1059 (2007)

Asymmetric Polymerizations of *N*-Substituted Maleimides Bearing L-Leucine Ester Derivatives and Chiral Recognition Abilities of Their Polymers

Tsutomu OISHI,† Huajing GAO, Taro NAKAMURA, Yukio ISOBE, and Kenjiro ONIMURA

Graduate School of Science and Engineering, Yamaguchi University, 2-16-1 Tokiwadai, Ube 755-8611, Japan

(Received April 27, 2007; Accepted July 8, 2007; Published August 28, 2007)

ABSTRACT: Two kinds of *N*-substituted maleimides bearing L-leucine ester derivatives ((*S*)-RLMI), *i.e.* (*S*)-*N*-maleoyl-L-leucine methyl ester ((*S*)-MLMI) and (*S*)-*N*-maleoyl-L-leucine benzyl ester ((*S*)-BnLMI), were synthesized from maleic anhydride, L-leucine, and corresponding alcohols. Asymmetric polymerizations were carried out to obtain optically active polymers. Specific rotations of the poly (RLMI)s were influenced by *N*-substituents, initiators, solvents and temperature. Chiroptical properties and structures of the poly((*S*)-RLMI)s obtained were investigated by GPC, CD, and NMR measurements. Optical activities of the poly((*S*)-RLMI)s obtained with anionic polymerization were attributed to excessive chiral centers of the main chain induced through the polymerizations in addition to the chirality of the *N*-substituents. The chiral stationary phases (CSPs) for high performance liquid chromatography (HPLC) were prepared and the chiral recognition abilities of the optically active poly((*S*)-RLMI)s were also discussed.
[doi:10.1295/polymj.PJ2007022]

KEY WORDS Maleimide / Chiral Recognition Ability / Leucine / Optically Active Polymer / Asymmetric Polymerization / Chiroptical Properties / Chiral Stationary Phase /

The synthesis of optically active polymer is an important field in macromolecular science because of a wide variety of potential applications based on the chiral structure, such as constructing chiral media for asymmetric synthesis; chiral stationary phases for resolution of enantiomers in chromatographic techniques; chiral liquid crystals in ferroelectrics and nonlinear optical devices.[1–4] Therein, the stationary phase for chiral high-performance-liquid-chromatography separation is one of the most successful applications of optically active polymers.[5–8] Thus, great attentions are paid to the syntheses of optically active polymers capable of chiral recognition.

According to the previous researches,[9,10] optically active polymers are synthesized either by the polymerization of monomers having an optically active moiety without chiral induction to the polymer chain or by polymerization in which chirality is introduced into the polymer structure through the asymmetric polymerization reaction. Chiral induction can be achieved either by catalytic reaction by using achiral or chiral monomers or by non-catalytic reaction systems typically based on chiral monomer structure. As one of useful methods, asymmetric synthesis polymerization can produce the polymers with configurational chirality of the main chain from an optically inactive, prochiral monomer or a prochiral monomer bearing an optically active auxiliary.

In the past decades, Oishi *et al.* have systematically researched asymmetric polymerizations of achiral or chiral *N*-substituted maleimides (RMIs) to obtain optically active polymers and optical resolution abilities of the poly(RMI)s obtained.[11–33] In 1991, Oishi *et al.* reported their first research on asymmetric anionic polymerizations of eleven types of achiral RMIs (*N*-substitutent (R) = *n*-propyl (PMI), isopropyl (IPMI), *n*-butyl (NBMI), isobutyl (IBMI), *s*-butyl (SBMI), *t*-butyl (TBMI), cyclohexyl (CHMI), benzyl (BZMI), phenyl (PhMI), 1-naphthyl (1-NMI), and 2-fluorenyl (FMI)) with *n*-BuLi/(−)-Sparteine (Sp) complex as initiator.[12] In these poly(RMI)s, poly(CHMI) showed the highest specific rotation ($[\alpha]_D^{25} = ca.\ -40^\circ$). Achiral *N*-glycinylmaleimide (GMI) and *N*-substituted maleimide having glycine ester derivative from glycine (achiral amino acid) have also been synthesized and their polymers have not been found showing chiral recognition abilities.[31,32] Besides the above researches on achiral RMIs, asymmetric polymerizations of chiral RMIs bearing chiral amine, such as (*R*)-*N*-α-methylbenzylmaleimide ((*R*)-(−)-MBZMI),[20] (*S*)-*N*-α-methylbenzylmaleimide ((*S*)-(−)-MBZMI),[21] (*S*)-*N*-1-cyclohexylethylmaleimide ((*S*)-CEMI),[28] (*R*)-*N*-1-cyclohexylethylmaleimide ((*R*)-CEMI),[28] and (*S*)-*N*-1-naphthylethylmaleimide ((*S*)-NEMI)[33] were also carried out, and polymers with higher specific rotations were obtained. Chiral RMIs are being expected to provide high optically active polymers because of their new chiralities of main chains in addition to the chiralities of *N*-substituents. Amino acids are important and useful substances for chiral auxilia-

†To whom correspondence should be addressed (Tel: +81-836-85-9281, Fax: +81-836-85-9201, E-mail: oishi@yamaguchi-u.ac.jp).

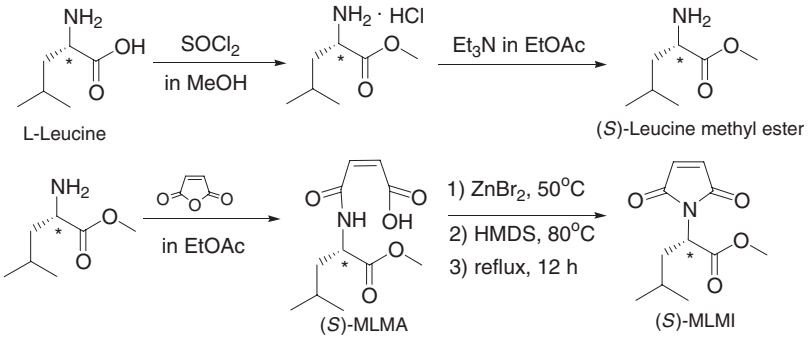

Scheme 1. Synthesis of (*S*)-MLMI

ries and building blocks in organic syntheses.[34,35] Because the varieties of chiral amino acids are very abundance, we can design some new chiral RMIs by introducing expected chiral amino acid to the *N*-substituent of maleimide and other various substituents are introduced to the carboxyl group of the side amino acid group in the RMI. From this point of view, Oishi *et al.* have chosen some chiral amino acids, such as L-alanine, L-phenylalanine, L-valine, D-phenylglycine and so on, as experimental subjects and reported the syntheses and asymmetric polymerizations of *N*-maleoyl-L-phenylalanine alkyl ester,[14,15] *N*-maleoyl-L-alanine ester (RAM),[16] chiral (*S*)-*N*-maleoyl-L-valine methyl ester ((*S*)-MVMI),[27] chiral (*R*)-*N*-maleoyl-D-phenylglycine alkyl ester.[29] At the same time, the researches have also been reported about the applications of poly(RMI)s on optical resolutions of racemates by being used as CSPs for HPLC.[29,33,36] Several racemates were resolved by the CSPs prepared from the corresponding polymers.

Very recently, we have published the asymmetric polymerizations of (*S*)-*N*-maleoyl-L-leucine propargyl ester[37,38] and (*S*)-*N*-maleoyl-L-leucine allyl ester,[39] both of which having an unsaturated reactive group in the side ester group of RMI. The optical resolutions of the chemically bonded-type chiral stationary phases (CSPs) using their polymers were also discussed. This time, we choose L-leucine as chiral amino acid and respectively introduce methyl group and benzyl group to the carboxyl group of L-leucine to extend our research width. In this work, we describe syntheses and asymmetric polymerizations of (*S*)-*N*-maleoyl-L-leucine methyl ester ((*S*)-MLMI) and (*S*)-*N*-maleoyl-L-leucine benzyl ester ((*S*)-BnLMI)—other two kinds of RMIs bearing L-leucine ester derivatives, and the applications of theirs polymers as CSPs for HPLC. Chiroptical properties and structures of these polymers were investigated in detail on the basis of measurements of nuclear magnetic resonance (NMR), specific optical rotations, circular dichroism (CD), and gel permeation chromatography (GPC). Furthermore, the HPLC analyses for separations of racemates using the CSPs prepared from the polymers are carried out. Chiral recognition abilities of the polymers are discussed.

EXPERIMENTAL

Reagents

Solvents used for syntheses, polymerizations, and measurements were purified in the usual manner. Commercially available *n*-butyllithium (*n*-BuLi) (Kanto Chemical Co., Inc., in *n*-hexane solution, 1.55 mol/L), dimethylzinc (Me_2Zn) (Kanto Chemical Co., in *n*-hexane solution, 1.00 mol/L) were used without further purification. Diethylzinc (Et_2Zn) was kindly supplied from Tosoh Corporation, and diluted with purified *n*-hexane (0.82 mol/L). (−)-Sparteine (Sp) (Tokyo Chemical Industry Co., Ltd.) was used after purification by distillation under reduced pressure ($[\alpha]_{435} = -10.3^\circ$ ($c = 1.0$ g/dL, $l = 10$ cm, THF)). (*S*,*S*)-(1-Ethylpropylidene)bis(4-benzyl-2-oxazoline) (Bnbox, $[\alpha]_{435} = -150.7^\circ$ ($c = 1.0$ g/dL, $l = 10$ cm, THF)) was prepared according to the published literature.[40] Radical initiator, 2,2′-azobisisobutyronitrile (AIBN) (Ishizu Seiyaku, Ltd.) was purified by recrystallization from methanol. Palladium-activated carbon (Wako Pure Chemical Industries, Ltd., Pd 10%) was used as purchased. Microporous silica gel (Si-100, pore size 100 Å, mean particle size 5 μm) and racemates were kindly supplied from Tosoh Corporation and used without further purification.

Synthesis of Monomer ((S)-MLMI)

Synthetic route of (*S*)-MLMI is shown in Scheme 1. Thionyl chloride ($SOCl_2$) (39.8 mL, 0.55 mol) was added dropwise to methanol (MeOH) (200 mL) in a three-neck flask at −10 °C. Then L-leucine (20.0 g, 0.15 mol) was added slowly to this solution at the same temperature. The mixture was stirred for 15 h at room temperature. After reaction, methanol and excess thionyl chloride were removed by distillation under reduced pressure. The residue was crystallized from diethyl ether. After filtered and dried under

vacuum, (*S*)-leucine methyl ester hydrochloride was obtained as a white powder [yield: 27.0 g (97.5%)].

(*S*)-Leucine methyl ester hydrochloride (10.0 g, 55.0 mol) was suspended into ethyl acetate (EtOAc) (100 mL). Triethylamine (Et_3N) (6.8 mL, 48.3 mol), which was dissolved in ethyl acetate (50 mL), was dropwise added into the mixture. After stirred over 10 minutes, it was collected by suction filtration. Maleic anhydride (5.4 g, 55.0 mol) was dissolved into ethyl acetate (50 mL), and then added into the above filtrate at room temperature. After stirred over 24 h, the mixture was fully washed by H_2O, saturated brine, and dried over Na_2SO_4. The above solution was concentrated by rotary evaporator to obtain (*S*)-maleamic acid-L-leucine methyl ester ((*S*)-MLMA) as white powder [yield: 11.5 g (85.6%), mp.: 90.0∼91.0 °C.].

(*S*)-MLMA (7.5 g, 31.0 mmol) was dissolved in benzene (200 mL) and put into a three-neck flask. Celite 545 (3.0 g) was added into the solution. After the solution was heated to 50 °C, $ZnBr_2$ (7.0 g, 31.0 mmol) was added. Then the solution of 1,1,1,3,3,3-hexamethyldisilazane (HMDS) (9.7 mL, 46.0 mmol) in benzene (50 mL) was added dropwise into the reaction mixture at 80 °C, and kept at this temperature for 12 h with stirring. The insoluble part in benzene was filtered off, and the filtrate was concentrated. The residue was dissolved into ethyl acetate and washed with 0.1 N HCl aq., saturated $NaHCO_3$, and then saturated brine. After dried over Na_2SO_4 and concentrated by rotary evaporator, crude product was obtained. Then purified further by column chromatography (eluent solvent: *n*-hexane/EtOAc = 1:1) and vacuum distillation with Kugelrohr apparatus, (*S*)-MLMI was obtained as white powder [yield: 4.4 g (62.9%), mp.: 62.0 °C, $[\alpha]_{435} = -35.5^\circ$ ($c = 1.0$ g/dL, $l = 10$ cm, THF) (lit.[41] $[\alpha]_D = -13.0^\circ$ ($c = 0.1$, CH_2Cl_2)]. ^{1}H NMR (δ in ppm from TMS in $CDCl_3$): 6.74 (2H, s, -CH=CH-), 4.76 (1H, t, -C*H), 3.72 (3H, s, -O-$\underline{C}H_3$), 2.21 and 1.86 (2H, m, -CH_2-), 1.41 (1H, m, -CH), 0.92 (6H, d, -CH_3). ^{13}C NMR (δ in ppm from TMS in $CDCl_3$): 20.86, 23.04 (-CH_3), 25.00 (-$\underline{C}H(CH_3)_2$), 37.04 (-$\underline{C}H_2$-), 50.53 ($\underline{C}H_3OCO$-), 52.69 (-$\underline{C}$*H=), 134.23 (-$\underline{C}H$=$\underline{C}H$-), 170.12 (-$\underline{C}OOCH_3$), 170.15 ($\underline{C}$=O).

Synthesis of Model Compound (S)-N-Succinoyl-L-leucine Methyl Ester ((S)-MLSI)

The synthetic route is shown in Scheme 2. (*S*)-MLMI (0.3 g, 1.33 mmol) was dissolved in ethyl acetate (10 mL) in a Schlenk reaction tube, and 10% palladium-activated carbon (0.030 g, 1 wt % to (*S*)-MLMI) was added to the solution. The reaction mixture was evacuated by aspirator and replaced by hydrogen gas 5 times. After stirred under hydrogen atmosphere for 15 h, the reaction tube was evacuated

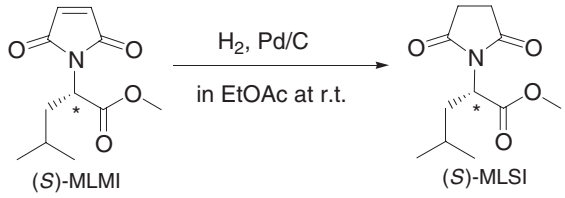

Scheme 2. Synthesis of (*S*)-MLSI

by an aspirator and replaced by nitrogen gas. Then the reaction mixture was filtered to remove palladium-activated carbon. The filtrate was concentrated under pressure to afford (*S*)-*N*-succionyl-L-leucine methyl ester ((*S*)-MLSI) as a white solid [yield: 0.30 g (99.7%), mp.: 39.2 °C, $[\alpha]_{435} = -120.3^\circ$ ($c = 1.0$ g/dL, $l = 10$ cm, THF)]. ^{1}H NMR (δ in ppm from TMS in $CDCl_3$): 4.80 (1H, t, -C*H), 3.72 (3H, s, -O-CH_3), 2.79 (4H, s, -CH_2-CH_2-), 2.18–1.90 (2H, m, -CH_2-), 1.41 (1H, m, -CH), 0.92 (6H, d, -CH_3). ^{13}C NMR (δ in ppm from TMS in $CDCl_3$): 176.50 (C=O in imide ring), 169.76 (C=O in ester group), 52.72 ($\underline{C}H_3OCO$), 51.05 (-C*H), 36.35 (-CH_2-), 28.03 (-$\underline{C}H_2$-$\underline{C}H_2$-), 25.02 (-$\underline{C}H(CH_3)_2$), 23.06 (-CH_3), 21.08 (-CH_3).

Synthesis of Monomer ((S)-BnLMI)

Synthetic route of (*S*)-BnLMI is shown in Scheme 3. L-Leucine (15.0 g, 0.11 mol), benzyl alcohol (57.0 mL, 0.55 mol), and *p*-toluenesulfonic acid (*p*-TsOH) (23.61 g, 0.14 mol) were suspended into benzene in a flask and refluxed 5 h. After reaction, the mixture was concentrated at reduced pressure and crystallized from diethyl ether. (*S*)-Leucine benzyl ester *p*-toluenesulfonate was obtained by filtering and drying as white powder (yield: 43.3 g (100%)). Then the obtained (*S*)-leucine benzyl ester *p*-toluenesulfonate (43.3 g, 0.11 mol) was suspended into ethyl acetate (200 mL), and the solution of triethylamine (6.8 mL, 48.3 mmol) in ethyl acetate (50 mL) was added dropwise into the mixture at room temperature. The reaction mixture was filtered. A solution of maleic anhydride (5.0 g, 51.0 mmol) in ethyl acetate (50 mL) was added dropwise into the above filtrate at room temperature and stirred 24 h. The reaction mixture was washed with water, saturated brine, and dried over Na_2SO_4, then concentrated under reduced pressure and (*S*)-*N*-leucine benzyl ester maleamic acid ((*S*)-BnLMA) was obtained as a white solid (yield: 29.9 g (82.0%), mp.: 105.0∼106.6 °C.). ^{1}H NMR (δ in ppm from TMS in $CDCl_3$): 7.35 (5H, m, phenyl), 6.35 (2H, dd, -CH=CH-), 4.73 (1H, m, -C*H), 1.52–1.82 (2H, m, -CH_2-) (1H, m, -CH), 0.95 (6H, m, -CH_3). ^{13}C NMR (δ in ppm from TMS in $CDCl_3$): 21.60 (-CH_3), 22.63 (-CH_3), 24.80 (-$\underline{C}H(CH_3)$), 40.43 (-CH_2-), 51.95 (-C*H), 67.46 (-CH_2-), 128.16,

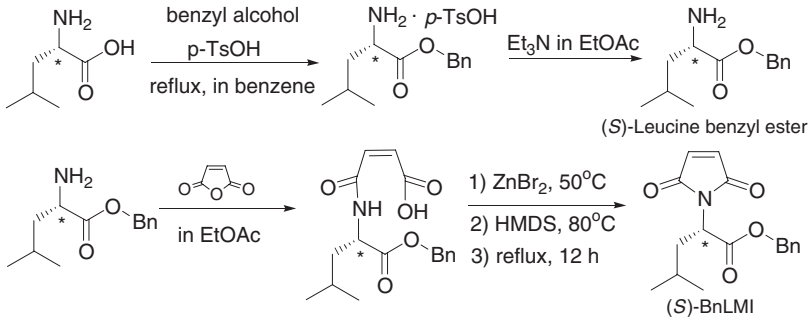

Scheme 3. Synthesis of (*S*)-BnLMI

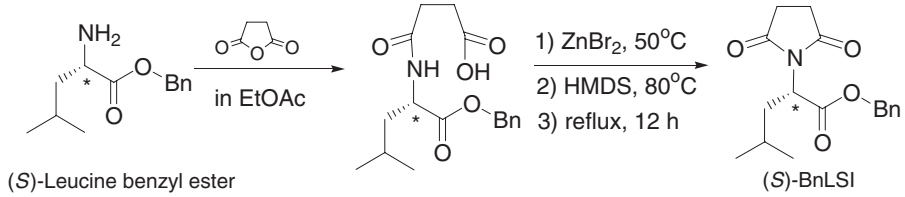

Scheme 4. Synthesis of (*S*)-BnLSI

128.52, 128.61, 131.29 (phenyl), 134.95, 136.37 (-CH=CH-), 165.62 (-COO-), 166.16 (-COO-), 171.36 (C=O).

Then (*S*)-BnLMI was synthesized from (*S*)-BnLMA instead of (*S*)-MLMA in a manner similar to (*S*)-MLMI. And purified further by column chromatography (eluent solvent: *n*-hexane/EtOAc = 4:1) and vacuum distillation with Kugelrohr apparatus, (*S*)-BnLMI was obtained as white powder (yield: 63.7%, mp.: 54.5 °C, $[\alpha]_{435} = -61.3^\circ$ ($c = 1.0$ g/dL, $l = 10$ cm, THF)). ^{1}H NMR (δ in ppm from TMS in $CDCl_3$): 7.18–7.35 (5H, m, phenyl), 6.67 (2H, s, -CH=CH-), 5.09 (2H, s, O-CH_2-), 4.74 (1H, t, -C*H), 2.21–1.84 (2H, m, -CH_2-), 1.39 (1H, m, -CH), 0.86 (6H, d, -CH_3). ^{13}C NMR (δ in ppm from TMS in $CDCl_3$): 20.86 (-CH_3), 23.06 (-CH_3), 25.03 (-CH(CH_3)), 36.98 (-CH_2-), 50.75 (-C*H), 67.48 (-CH_2-C_6H_5), 128.07, 128.36, 128.55 (phenyl), 134.23, 135.18 (-CH=CH-), 165.60 (-COO-), 170.13 (C=O).

Synthesis of Model Compound (S)-N-Succinoyl-L-leucine Benzyl Ester ((S)-BnLSI)

The synthetic route was shown in Scheme 4. (*S*)-*N*-Succinoyl-L-leucine benzyl ester ((*S*)-BnLSI) was synthesized from (*S*)-leucine benzyl ester and succinic anhydride by the same method as (*S*)-BnLMI (yield: 21.6%, mp.: 109.2 °C, white acicular crystal, $[\alpha]_{435} = -112.1^\circ$ ($c = 1.0$ g/dL, $l = 10$ cm, THF)). ^{1}H NMR (δ in ppm from TMS in $CDCl_3$): 7.29–7.52 (5H, m, phenyl), 5.15 (2H, s, O-CH_2-), 4.85 (1H, t, -C*H), 4.73 (4H, s, -CH_2-CH_2-), 2.21–1.94 (2H, m, -CH_2-), 1.41 (1H, m, -CH), 0.95 (6H, d, -CH_3). ^{13}C NMR (δ in ppm from TMS in $CDCl_3$): 21.40 (-CH_3), 23.00 (-CH_3), 25.39 (-CH(CH_3)), 28.35 (-CH_2-CH_2-), 36.61 (-CH_2-), 51.61 (-C*H), 67.80 (-CH_2-C_6H_5), 128.48, 128.70, 128.90 (phenyl), 165.43 (-COO-), 176.84 (C=O).

Polymerization

All experiments for polymerization reactions were carried out under purified nitrogen atmosphere to exclude oxygen and moisture. Anionic polymerizations were carried out in the following procedures. Monomer and chiral ligand were put in a Schlenk reaction tube and a pear-sharped flask, then evacuated by vacuum pump, and replaced by dry nitrogen gas 5 times. Polymerization solvent (THF or toluene) was added to each vessel by a syringe under nitrogen atmosphere to dissolve them. Organomental (*n*-BuLi, Me_2Zn, or Et_2Zn) in *n*-hexane solution was introduced into the chiral ligand solution with a syringe to prepare the initiator complex. While the monomer solution was kept at polymerization temperature, the complex solution was added by a cannula in a stream of nitrogen gas to initiate polymerization. After prescribed time, polymerization was terminated with a small amount of methanol containing 2 drops of 6 N hydrochloric acid. The solution was poured into a large amount of methanol to precipitate polymer, which was then collected by suction filtration, washed with methanol, and dried. Purification of the polymers was achieved by reprecipitation in a THF-methanol system. The obtained polymer was dried under vacuum at room temperature for 2 d before measurements.

Radical polymerization was conducted with AIBN as an initiator in THF or toluene in a sealed tube at

60 °C for 24 h. After polymerization, the solution was poured into a large amount of methanol to precipitate the polymer. The obtained product was purified by reprecipitation twice from THF-methanol system, filtered and dried under vacuum at room temperature for 2 d.

Preparation of CSP for HPLC and Column Packing

Optically active poly((*S*)-RLMI) (0.035 g) was dissolved in chloroform (20 mL). Microporous silica gel (Si-100, 0.70 g) was added to the solution of polymer. After irradiation with ultrasound for 5 min, the mixture was evaporated to dryness under reduced pressure to afford poly((*S*)-RLMI)-coated-silica gel (CSP).

Obtained CSP was dispersed in 2-propanol (10 mL) and packed into stainless steel HPLC columns by a high-pressure slurry packing technique using 2-propanol as packing solvent. Theoretical plate numbers of the columns were measured using toluene as standard in *n*-hexane/2-propanol (9/1, v/v) as eluent at a flow rate of 0.5 mL/min at 25 °C, according to the following equation:

$$N = 5.54 \times (t_r/w_{1/2})^2$$

where t_r is a retention time and $w_{1/2}$ is a half band width.

Measurements

Specific rotations were measured in THF at 25 °C using a quartz cell ($l = 10$ cm) with a JASCO DIP-140 polarimeter (JASCO Co. Ltd.). CD spectra were recorded in THF at 25 °C using a quartz cell of 1 mm with a JASCO J-805 spectropolarimeter (JASCO Co. Ltd.). Number-average molecular weights (M_ns) and polydispersity (M_w/M_ns) of polymers were determined by a gel permeation chromatography (GPC) using THF (50 °C) as an eluent and polystyrene as a standard on a Shimadzu LC-10A instrument equipped with a SPD-10A UV-vis detector, a polarimetric detector (JASCO OR-990), and a C-R7Ae plus data processor. ^{1}H (270 MHz) and ^{13}C NMR (68 MHz) spectra were measured on a JEOL-EX270 apparatus (JEOL, Ltd.). HPLC analysis was carried out with an apparatus consisting of a LC-10AT liquid chromatography (Shimadzu), a CTO-10AS column oven (Shimadzu), two CHROMATOPAC C-R8A (Shimadzu), a SPD-10A UV detector (254 nm) (Shimadzu), and a JASCO-OR 2090 polarimetric detector (350–900 nm).

RESULTS AND DISCUSSION

Polymerizations

Scheme 5 shows the anionic polymerization routes for (*S*)-MLMI and (*S*)-BnLMI.

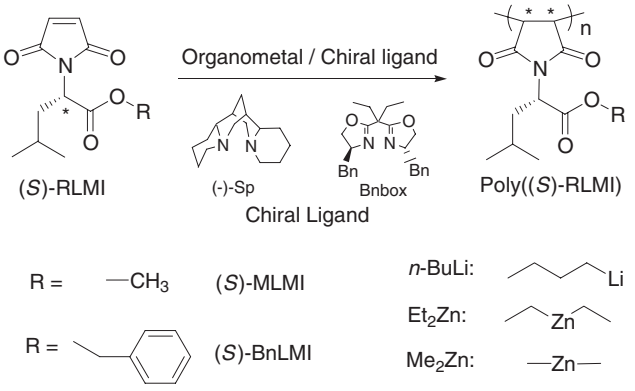

Scheme 5. Anionic polymerization of (*S*)-RLMI

Polymerizations of (S)-MLMI

Table I summarizes the conditions and results of the asymmetric anionic polymerizations of (*S*)-MLMI using *n*-BuLi, Et_2Zn, AIBN, *n*-BuLi/ligand, Et_2Zn/ligand, or Me_2Zn/ligand, as initiators. All polymerizations proceeded in the homogeneous system from beginning to end, and all of the polymers obtained were soluble in THF and $CHCl_3$. All of the polymers exhibited negative specific rotations. The yields of the methanol-insoluble part, the M_ns and specific rotations of poly((*S*)-MLMI)s were strongly affected by organometals, ligands, and temperature. In the anionic polymerization of (*S*)-MLMI with *n*-BuLi initiator series, the yields of methanol-insoluble part of poly((*S*)-MLMI)s obtained with ligand have a tendency to increase both in THF and toluene comparing with those obtained with *n*-BuLi only, but big changes were not observed in the aspect of the M_ns of polymers. It was the same tendency when used Et_2Zn initiator series. These results suggested that the catalytic activity of the organometal/ligand complex was higher than that of organometal. The coordination of the organometal with the ligand contributes to enhance the catalytic activity.

When decreased the ratio of ligand to Et_2Zn, the yields of poly((*S*)-MLMI) obtained with Et_2Zn/ligand (1.0/0.5) at 0 °C both decreased comparing with those obtained with Et_2Zn/ligand (1.0/1.2), while the M_ns of polymers increased. It was the same phenomenon with the polymerizations using Me_2Zn/ligand. This tendency was not observed for the polymerization under −40 °C.

The yields and M_ns of poly((*S*)-MLMI)s prepared with Et_2Zn/ligand complex or Me_2Zn/ligand complex were higher than those with *n*-BuLi/ligand complex under the same polymerization conditions. This may result from that the reactivity of the propagating species with dialkylzinc (Et_2Zn or Me_2Zn) is relatively higher than that with *n*-BuLi although the initiating reactivity of dialkylzinc is lower than *n*-BuLi. On the other hand, the M_ns of polymers (runs 15–16 in

Table I. Asymmetric Polymerizations of (*S*)-MLMI

Run	Initiator[b]	Solv.[c] (mL)	Temp. °C	Time h	Yield[d] %	M_n[e] $\times 10^{-4}$	M_w/M_n[e]	$[\alpha]_{435}$[f] deg.	$[\alpha]_D$[f] deg.
1	*n*-BuLi	THF (5)	0	24	36.6	1.56	1.27	−256.6	−124.6
2	*n*-BuLi	Tol. (5)	0	24	27.2	1.40	1.60	−144.4	−71.8
3	*n*-BuLi/Bnbox (1.0/1.2)	THF (5)	0	24	43.6	1.22	1.79	−336.0	−160.1
4	*n*-BuLi/Bnbox (1.0/1.2)	Tol. (5)	0	24	46.7	1.56	1.35	−283.3	−140.1
5	*n*-BuLi/Sp (1.0/1.2)	THF (5)	0	24	25.8	1.34	1.26	−330.6	−161.4
6	*n*-BuLi/Sp (1.0/1.2)	Tol. (5)	0	24	64.6	1.64	1.44	−279.6	−134.4
7	Et_2Zn	THF (5)	0	72	7.8	1.28	1.20	−2.1[h]	−1.9[h]
8	Et_2Zn	Tol. (5)	0	72	6.0	1.74	1.48	−136.6[h]	−72.4[h]
9	Et_2Zn/Bnbox (1.0/1.2)	THF (5)	0	72	64.2	1.64	1.66	−261.1[g]	−124.7[g]
10	Et_2Zn/Bnbox (1.0/1.2)	Tol. (5)	0	72	63.6	1.50	1.22	−144.7	−72.5
11	Et_2Zn/Bnbox (1.0/0.5)	Tol. (5)	0	72	55.8	1.54	1.30	−133.3[h]	−62.9[h]
12	Et_2Zn/Sp (1.0/1.2)	THF (5)	0	72	74.8	1.87	1.32	−234.6	−116.0
13	Et_2Zn/Sp (1.0/1.2)	Tol. (5)	0	72	64.9	1.36	1.54	−271.3	−131.7
14	Et_2Zn/Sp (1.0/0.5)	Tol. (5)	0	72	44.8	1.58	1.24	−310.0[h]	−145.4[h]
15	Me_2Zn/Sp (1.0/0.5)	Tol. (5)	0	72	45.5	2.66	1.38	−320.9	−156.4
16	Me_2Zn/Sp (1.0/1.2)	Tol. (5)	0	72	67.0	2.40	1.70	−221.1	−108.9
17	Et_2Zn/Sp (1.0/1.2)	Tol. (5)	−40	72	5.3	2.58	1.28	−92.6[h]	−60.4[h]
18	Et_2Zn/Sp (1.0/0.5)	Tol. (5)	−40	72	29.6	1.09	1.18	−454.7[i]	−220.1[i]
19	AIBN	THF (5)	60	24	0	—	—	—	—
20	AIBN	Tol. (5)	60	24	40.7	1.55	1.23	−92.8	−47.4

[a]Monomer: 0.5 g. [b][Organometal]/[Monomer] = 0.1, [AIBN]/[Monomer] = 0.1. [c]THF: tetrahydrofuran, Tol.: toluene. [d]Methanol-insoluble part. [e]By GPC. [f]$c = 1.0$ g/dL, $l = 10$ cm in THF. [g]THF-soluble part. [h]$c = 0.2$ g/dL, $l = 10$ cm in THF. [i]$c = 0.1$ g/dL, $l = 10$ cm in $CHCl_3$.

Table I) obtained with Me_2Zn/Sp were higher than those with Et_2Zn/ligand (runs 9–14 in Table I). This is probably attributed to the fact that the complex of Me_2Zn/Sp has higher nucleophilicity to prompt the growing of ion pair than the complex of Et_2Zn/ligand and the propagation rate increases when used less bulky Me_2Zn in the polymerization.

When the anionic polymerization was performed at −40 °C, the yields of poly((*S*)-MLMI) (runs 17–18 in Table I) decreased comparing with the polymers (runs 13–14 in Table I) obtained under the same conditions at 0 °C. This may be attributed to decreasing reactive activity of the initiator and/or the poor propagating rate of growing polymer at low temperature.

The radical polymerization of (*S*)-MLMI was performed in toluene (run 20 in Table I), and did not proceed in THF (run 19 in Table I). The polarity of solvent obviously affects the radical polymerizability of (*S*)-MLMI.

Polymerizations of (S)-BnLMI

Table II summarizes the conditions and results of the asymmetric polymerizations of (*S*)-BnLMI using organometal (*n*-BuLi or Et_2Zn), AIBN, or organometal/ligand (*n*-BuLi/ligand, Et_2Zn/ligand, or Me_2Zn/ligand), as initiators. All polymerizations proceeded in the homogeneous system from beginning to end, and all of the polymers obtained were soluble in THF and $CHCl_3$. As the same as (*S*)-MLMI, the yields of the methanol-insoluble part, the M_ns and specific rotations of poly((*S*)-BnLMI)s were also strongly affected by organometals, ligands, and temperature. In the anionic polymerization of (*S*)-BnLMI used *n*-BuLi/ligand complex as initiator, the yields of methanol-insoluble part and M_ns of poly((*S*)-BnLMI)s obtained in toluene increased comparing with those obtained in THF. When Et_2Zn/ligand complex was used as initiator, the M_ns of polymers obtained in THF were higher than those obtained in toluene. This is the same tendency as poly((*S*)-MLMI). It may be attributed to the coordination between the oxygen of THF and Et_2Zn/ligand complex to form Et_2Zn/THF/ligand complex.

When decreased the ratio of ligand to Et_2Zn, the change tendency of the yields and M_ns of poly((*S*)-BnLMI) obtained with Et_2Zn/ligand (1.0/0.5) at 0 °C was not obvious comparing with those obtained with Et_2Zn/ligand (1.0/1.2). The M_ns of poly((*S*)-BnLMI)s (runs 15–16 in Table II) obtained with Me_2Zn/Sp were greater than those with Et_2Zn/ligand (runs 7–14 in Table II). When the anionic polymerization was performed at −40 °C, the yields of poly((*S*)-BnLMI) (run 17 in Table II) decreased comparing with the polymers (run 7 in Table II) obtained under the same conditions at 0 °C. These are the same as poly((*S*)-MLMI).

Table II. Asymmetric Polymerizations of (*S*)-BnLMI

Run	Initiator[b]	Solv.[c] (mL)	Temp. °C	Time h	Yield[d] %	M_n[e] $\times 10^{-4}$	M_w/M_n[e]	$[\alpha]_{435}$[f] deg.	$[\alpha]_D$[f] deg.
1	*n*-BuLi	THF (5)	0	24	66.4	0.78	1.54	−202.5	−101.0
2	*n*-BuLi	Tol. (5)	0	24	59.4	0.60	1.65	−50.6	−25.6
3	*n*-BuLi/Bnbox (1.0/1.2)	THF (5)	0	24	49.4	0.49	1.43	−162.5	−74.3
4	*n*-BuLi/Bnbox (1.0/1.2)	Tol. (5)	0	24	85.5	0.91	2.11	−195.7	−95.6
5	*n*-BuLi/Sp (1.0/1.2)	THF (5)	0	24	60.2	0.85	1.54	−157.2[g]	−82.3[g]
6	*n*-BuLi/Sp (1.0/1.2)	Tol. (5)	0	24	80.1	1.02	1.66	−239.4	−115.3
7	Et_2Zn/Sp (1.0/1.2)	THF (5)	0	72	93.0	1.68	1.93	−12.2	−7.8
8	Et_2Zn/Sp (1.0/1.2)	Tol. (5)	0	72	79.0	0.99	1.79	−109.0	−54.8
9	Et_2Zn/Sp (1.0/0.5)	THF (5)	0	72	26.8	2.22	2.47	−34.5	−18.3
10	Et_2Zn/Sp (1.0/0.5)	Tol. (5)	0	72	83.0	0.75	1.65	−97.4	−49.1
11	Et_2Zn/Bnbox (1.0/1.2)	THF (5)	0	72	69.9	1.36	1.62	−103.6	−54.0
12	Et_2Zn/Bnbox (1.0/1.2)	Tol. (5)	0	72	73.0	0.98	1.56	−6.7	−7.4
13	Et_2Zn/Bnbox (1.0/0.5)	THF (5)	0	72	81.6	1.27	1.70	−84.4	−43.4
14	Et_2Zn/Bnbox (1.0/0.5)	Tol. (5)	0	72	75.7	0.96	1.59	+42.4	+15.0
15	Me_2Zn/Sp (1.0/1.2)	THF (5)	0	72	51.6	3.16	2.89	−58.2	−31.3
16	Me_2Zn/Bnbox (1.0/0.5)	THF (5)	0	72	29.6	2.47	2.58	−74.2	−36.5
17	Et_2Zn/Sp (1.0/1.2)	THF (5)	−40	72	6.0	1.31	1.29	+139.3[h]	+67.5[h]
18	AIBN	Tol. (5)	60	24	70.2	0.58	1.58	−58.2	−30.1

[a]Monomer: 0.5 g. [b][Organometal]/[Monomer] = 0.1, [AIBN]/[Monomer] = 0.1. [c]THF: tetrahydrofuran, Tol.: toluene. [d]Methanol-insoluble part. [e]By GPC. [f]$c = 1.0$ g/dL, $l = 10$ cm in THF. [g]$c = 1.0$ g/dL, $l = 10$ cm in $CHC1_3$. [h]$c = 0.09$ g/dL, $l = 10$ cm in THF.

The radical polymerization of (*S*)-BnLMI was performed in toluene (run 18 in Table II) and the M_n of polymer obtained was relatively lower.

Chiroptical properties of polymers

Chiroptical Property of Poly((S)-MLMI). All the poly((*S*)-MLMI)s obtained were levorotatory. The highest specific rotation of poly((*S*)-MLMI) was obtained with Et_2Zn/Sp in toluene (run 18 in Table I, $[\alpha]_{435} = -454.7°$). Most polymers obtained from anionic polymerizations had higher specific rotations than model compound ($[\alpha]_{435} = -120.3°$) except for runs 7 and 17 in Table I. This is ascribed to the new asymmetric induction in the main chains of most polymers. For the *n*-BuLi initiator series, the polymer obtained in THF had higher specific rotation than in toluene. But for the Et_2Zn initiator series, the polymer obtained in toluene had the tendency of having higher specific rotation than those in THF. The specific rotations of polymers obtained with *n*-BuLi or *n*-BuLi/ligand complexes were much more shifted to levorotatory than those with Et_2Zn or Et_2Zn/ligand complex under the same polymerization conditions. This tendency could be attributable to the difference of structures between counter metal cations at the propagating chain end. The polymers with high negative specific rotations would possess (*R*,*R*)-main-chain configuration more than (*S*,*S*)-one, judging from the previous researches found by some of the authors.[17,24]

CD and UV spectra were determined to get information about chiroptical properties of optically active poly((*S*)-MLMI). Typical CD and UV spectra of (*S*)-MLMI, (*S*)-MLSI, and poly((*S*)-MLMI)s obtained by anionic, and radical polymerizations are depicted in Figure 1. The UV absorptions of poly((*S*)-MLMI)s appeared at the same position as the (*S*)-MLMI and (*S*)-MLSI. The CD spectra of both (*S*)-MLMI and (*S*)-MLSI exhibited positive Cotton effect around 230–260 nm (curves 1 and 2 in Figure 1), which was mainly attributable to the n-π^* electron transition of carbonyl groups in *N*-substituent. In the CD spectra of poly((*S*)-MLMI)s obtained by anionic polymerization, the spectral pattern was changed with the specific rotation of the polymer. For *n*-BuLi initiator series, the relative intensities of the CD spectra decreased with the shift of specific rotations toward negative (curves 4–6 in Figure 1). As levorotation of poly((*S*)-MLMI) increased, the positive Cotton effect around 230–260 nm shifted to zero. While for Et_2Zn initiator series, the relative intensities of the CD spectra also decreased with the shift of specific rotations toward negative (curves 7–9 in Figure 1) with different degree comparing with those in *n*-BuLi initiator series. These indicated that the new negative CD peak induced by carbonyl groups in the maleimide moiety appeared in the same wavelength region in an addition to the intrinsic CD peak due to chiral *N*-substituent. These results demonstrate that poly((*S*)-MLMI)s possess asymmetric carbons not only in the *N*-substituent, but also in the main chain. At the same time, the induced stereoregularities of the polymers were different for *n*-BuLi initiator series and Et_2Zn initiator series.

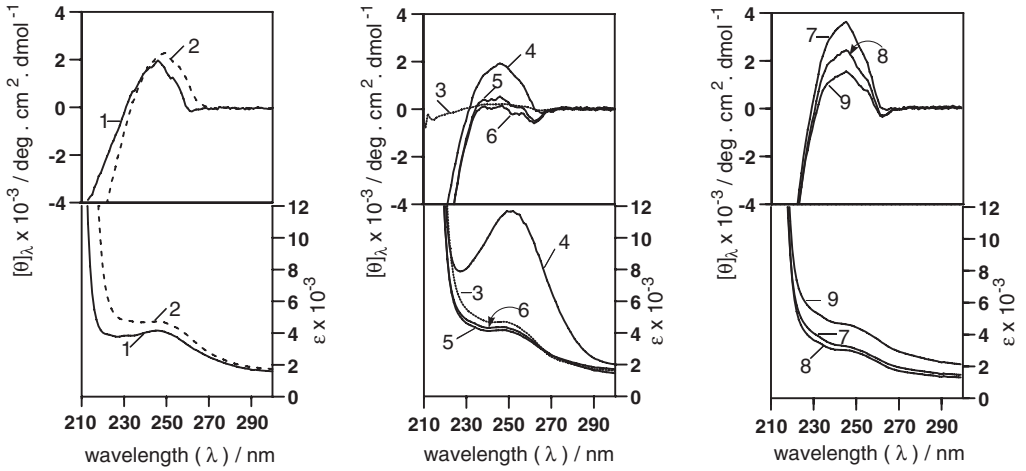

Figure 1. CD and UV spectra of (*S*)-MLMI (1, $[\alpha]_{435} = -34.9°$), (*S*)-MLSI (2, $[\alpha]_{435} = -120.3°$), and poly((*S*)-MLMI)s obtained with AIBN in toluene (3, $[\alpha]_{435} = -92.8°$, run 20 in Table I), *n*-BuLi in toluene (4, $[\alpha]_{435} = -144.4°$, run 2 in Table I), *n*-BuLi/Sp (1.0/1.2) in THF (5, $[\alpha]_{435} = -330.6°$, run 5 in Table I), *n*-BuLi/Bnbox (1.0/1.2) in THF (6, $[\alpha]_{435} = -336.0°$, run 3 in Table I), Et_2Zn/Bnbox (1.0/1.2) in toluene (7, $[\alpha]_{435} = -144.7°$, run 10 in Table I), Et_2Zn/Sp (1.0/1.2) in THF (8, $[\alpha]_{435} = -234.6°$, run 12 in Table I), and Et_2Zn/Sp (1.0/1.2) in toluene (9, $[\alpha]_{435} = -271.3°$, run 13 in Table I).

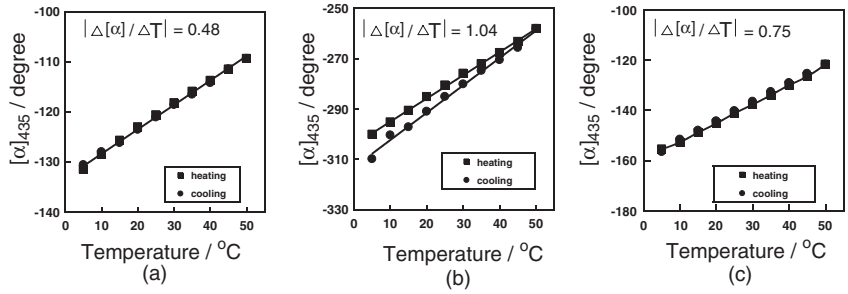

Figure 2. Effect of measurement temperature on specific rotation of (*S*)-MLSI (a, $[\alpha]_{435} = -120.3°$), and poly((*S*)-MLMI)s obtained with *n*-BuLi/Bnbox (1.0/1.2) in toluene (b, $[\alpha]_{435} = -283.3°$, run 4 in Table I), and Et_2Zn/Bnbox (1.0/1.2) in toluene (c, $[\alpha]_{435} = -144.7°$, run 10 in Table I).

Figure 2 displays the changes in the specific rotations of (*S*)-MISI and poly((*S*)-MLMI)s with temperature of measurement in THF. The absolute values of specific optical rotations linearly decreased with increasing temperature, and the changes are reversible. Comparing with the change of value temperature coefficient of model compound (*S*)-MLSI ($|\Delta[\alpha]/\Delta T| = 0.48$, (a) in Figure 2), the polymer having higher negative specific rotation ($[\alpha]_{435} = -283.3°$, (b) in Figure 2) showed the bigger change of value temperature coefficient ($|\Delta[\alpha]/\Delta T| = 1.04$) than the lower one ($[\alpha]_{435} = -144.7°$, (c) in Figure 2, $|\Delta[\alpha]/\Delta T| = 0.75$). These results indicated that other asymmetric inductions were induced in the main chains of poly((*S*)-MLMI)s in addition to the chirality of the *N*-subsituent and the decrease in specific optical rotation may be due to relaxation of partial helical conformations caused by heating.

Chiroptical property of poly((S)-BnLMI). The poly((*S*)-BnLMI)s obtained might be levorotatory and dextrotatory. The highest negative specific rotation of poly((*S*)-BnLMI) was obtained with *n*-BuLi/Sp in toluene (run 6 in Table II, $[\alpha]_{435} = -239.4°$) and the highest positive specific rotation ones was obtained with Et_2Zn/Sp in THF at $-40\,°C$ (run 17 in Table II, $[\alpha]_{435} = +139.3°$). Most polymers obtained with *n*-BuLi initiator series had higher specific rotations than model compound ($[\alpha]_{435} = -112.3°$) except for run 2 in Table II. But the effects of chiral ligands on promoting specific rotations of the polymers were not obvious. These indicated that new asymmetric inductions were induced in the main chains of most polymers and the asymmetric environment was mainly supplied by the chirality of *N*-substituent. But for the Et_2Zn and Me_2Zn initiator series, the specific rotations of the polymers obtained had the tendency of shifting to dextrotatory.

Information about chiroptical properties of optically active poly((*S*)-BnLMI)s was also given by CD and UV spectra. Typical CD and UV spectra of (*S*)-BnLMI, (*S*)-BnLSI, and poly((*S*)-BnLMI)s obtained by anionic and radical polymerizations are depicted

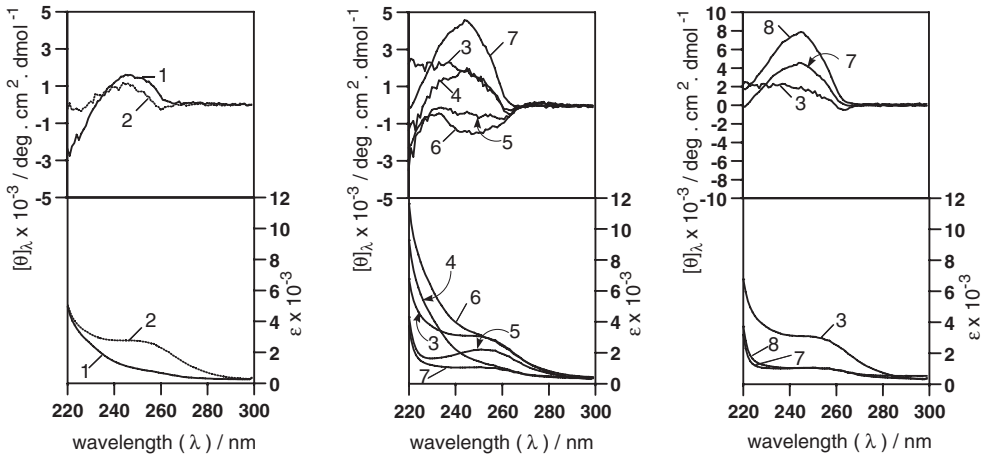

Figure 3. CD and UV spectra of (*S*)-BnLMI (1, $[\alpha]_{435} = -62.3^\circ$), (*S*)-BnLSI (2, $[\alpha]_{435} = -112.1^\circ$), and poly((*S*)-BnLMI)s obtained with AIBN in toluene (3, $[\alpha]_{435} = -58.2^\circ$, run 18 in Table II), Et_2Zn/Sp (1.0/1.2) in toluene (4, $[\alpha]_{435} = -109.0^\circ$, run 8 in Table II), *n*-BuLi in THF (5, $[\alpha]_{435} = -202.5^\circ$, run 1 in Table II), *n*-BuLi /Sp (1.0/1.2) in toluene (6, $[\alpha]_{435} = -239.4^\circ$, run 6 in Table II), Et_2Zn/Bnbox (1.0/1.2) in toluene (7, $[\alpha]_{435} = -6.7^\circ$, run 12 in Table II), Et_2Zn/Sp (1.0/1.2) in toluene (8, $[\alpha]_{435} = +139.3^\circ$, run 17 in Table II).

in Figure 3. The UV absorptions of poly((*S*)-BnLMI)s can be observed at the same position as the (*S*)-BnLMI and (*S*)-BnLSI. The CD spectra of both (*S*)-BnLMI and (*S*)-BnLSI exhibited positive Cotton effect around 230–260 nm (curves 1 and 2 in Figure 3), which was mainly attributable to the n-π^* electron transition due to carbonyl groups in *N*-substituent. In the CD spectra of poly((*S*)-BnLMI)s obtained by anionic polymerization, the spectral pattern was changed with the specific rotation of the polymer. The relative intensities of the positive Cotton effect of CD spectra decreased with the shift of specific rotations toward levorotatory (curves 4–6 in Figure 3) and negative Cotton effect was obviously seen in the CD spectrum of the polymer having the highest negative specific rotation -239.4° (curve 6 in Figure 3). While, when the specific rotation of polymer shifted toward dextrorotatory, the relative intensities of the positive Cotton effect of the CD spectra increased (curves 7–8 in Figure 3) and the biggest relative intensity of positive Cotton effect was displayed in the CD spectrum of the polymer having the highest positive specific rotation $+139.3^\circ$ (curve 8 in Figure 3). These indicated that the new CD peaks induced by carbonyl groups in the maleimide moiety appeared in the same wavelength region in an addition to the intrinsic CD peak due to chiral *N*-substituent. These results also demonstrate that the poly((*S*)-BnLMI)s with different specific rotation possess different induced stereoregularities belonging to the asymmetric carbons in the main chain.

The changes in the specific rotations of (*S*)-BnLSI and poly((*S*)-BnLMI)s with temperature of measurement in THF is shown in Figure 4. All of the absolute values of specific optical rotations linearly decreased

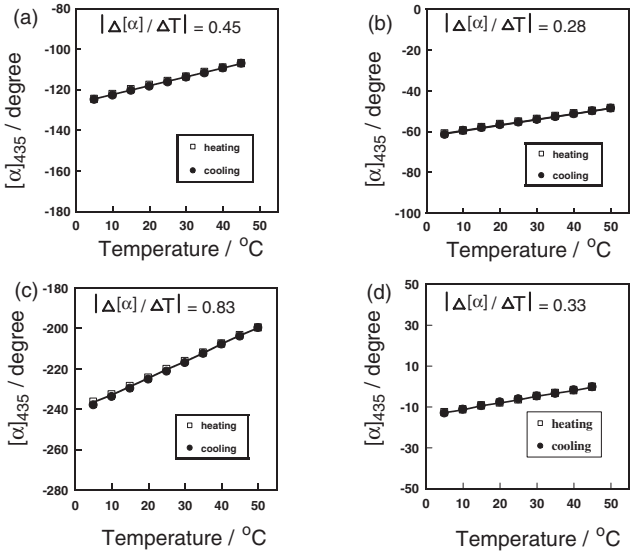

Figure 4. Effect of measurement temperature on specific rotation of (*S*)-BnLSI (a, $[\alpha]_{435} = -112.1^\circ$), and poly((*S*)-BnLMI)s obtained with *n*-BuLi in toluene (b, $[\alpha]_{435} = -50.6^\circ$, run 2 in Table II), *n*-BuLi/Bnbox (1.0/1.2) in toluene (c, $[\alpha]_{435} = -195.7^\circ$, run 4 in Table II), and Et_2Zn/Sp (1.0/1.2) in toluene (d, $[\alpha]_{435} = -6.7^\circ$, run 12 in Table II).

with increasing temperature, and the changes are reversible. Comparing with the change of value temperature coefficient of model compound (*S*)-BnLSI ($|\Delta[\alpha]/\Delta T| = 0.45$, (a) in Figure 4), the polymer having higher negative specific rotation ($[\alpha]_{435} = -195.7^\circ$, (c) in Figure 4) showed the bigger change of value temperature coefficient ($|\Delta[\alpha]/\Delta T| = 0.83$) than those having lower specific rotations ((b) in Figure 4, $[\alpha]_{435} = -50.6^\circ$, $|\Delta[\alpha]/\Delta T| = 0.28$; and (d) in Figure 4, $[\alpha]_{435} = -6.7^\circ$, $|\Delta[\alpha]/\Delta T| = 0.33$). When the specific rotations of polymers shift to posi-

tive direction, the values of temperature coefficients become small. This may be attributed to the counteraction of specific rotation-temperature value change between the chiralities coming from the *N*-substituent and the new asymmetric induction in the polymer main chain.

The typical GPC chromatograms of poly((*S*)-MLMI)s and poly((*S*)-BnLMI)s are shown in Figure 5. The top and bottom curves are obtained by polarimetric and UV detections, respectively. For the polymers obtained by anionic polymerization, both of the polarimetric chromatograms corresponded to those of UV. This indicates that every molecular weight part of the polymers possessed the equivalent optical rotation and the optical activities of the poly((*S*)-MLMI)s and poly((*S*)-BnLMI)s were independent of the molecular weight.

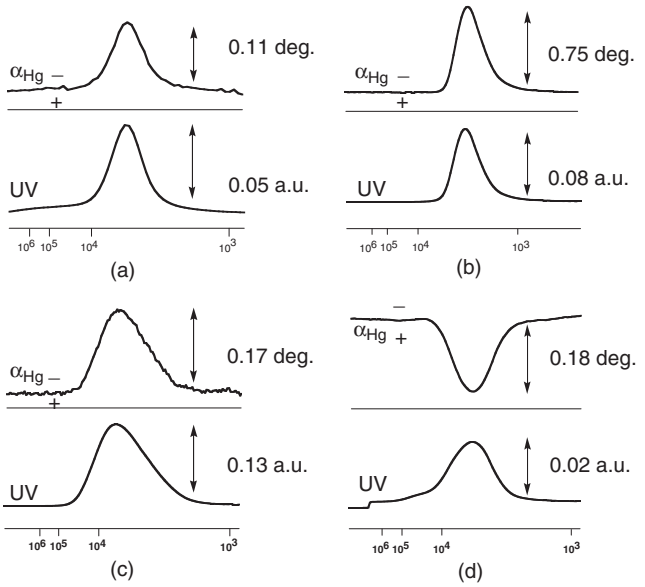

Figure 5. GPC chromatograms of poly((*S*)-MLMI)s (a, $[\alpha]_{435} = -336.0^\circ$, run 3 in Table I), (b, $[\alpha]_{435} = -454.7^\circ$, run 18 in Table I), and poly((*S*)-BnLMI)s (c, $[\alpha]_{435} = -109.0^\circ$, run 18 in Table II), (d, $[\alpha]_{435} = +139.3^\circ$, run 17 in Table II), monitored using UV (bottom curves) and polarmetric (α_{Hg}, top curves) detectors.

Structures of polymers

^{13}C NMR spectra were measured to obtain more structural information on poly((*S*)-RLMI).

Figure 6 shows typical ^{13}C NMR spectra of poly((*S*)-MLMI)s obtained with AIBN (a), *n*-BuLi/Bnbox (b), and Et_2Zn/Sp (c). All peaks of poly((*S*)-MLMI)s obtained in anionic polymerizations (b and c) were sharper than that obtained in radical polymerizations (a). The expanded spectra of polymer for main chain (40–48 ppm), carbonyl of side chain (166–171 ppm), and carbonyl of imide ring (174–178 ppm) are also shown in Figure 6. The difference in signals can be obviously confirmed in the expanded main chain peaks. Based on our previous researches,[12,16,19,42,43] the peaks at lower magnetic field (about 45–43.5 ppm) and higher one (about 43–40 ppm) are assigned to *threo*-disyndiotactic and *threo*-diisotactic structures of the main chain, respectively. Poly((*S*)-MLMI)s obtained with anionic polymerization (b and c in Figure 6) exhibited clear peaks belonging to the *threo*-diisotactic structures in the main chain region. This indicates that poly((*S*)-MLMI)s prepared by anionic polymerization possess higher stereoregularity.

Figure 7 shows typical ^{13}C NMR spectra of poly((*S*)-BnLMI)s obtained with *n*-BuLi/Sp (a), Et_2Zn/Sp (b), and AIBN (c). All peaks of poly((*S*)-BnLMI)s obtained in anionic polymerizations (a and b) were sharper than that obtained in radical polymer-

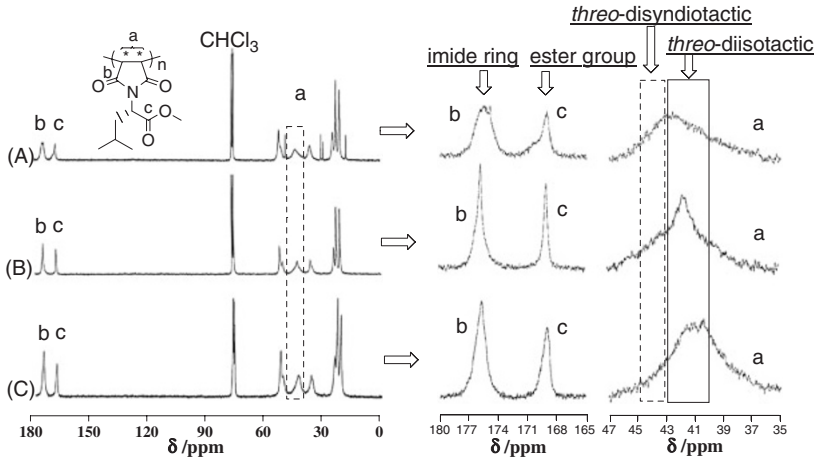

Figure 6. ^{13}C NMR spectra of poly((*S*)-MLMI)s obtained with AIBN in toluene ((A), $[\alpha]_{435} = -92.8^\circ$, run 20 in Table I), *n*-BuLi/Bnbox (1.0/1.2) in THF ((B), $[\alpha]_{435} = -336.0^\circ$, run 3 in Table I), Et_2Zn/Sp (1.0/1.2) in toluene ((C), $[\alpha]_{435} = -271.3^\circ$, run 13 in Table I).

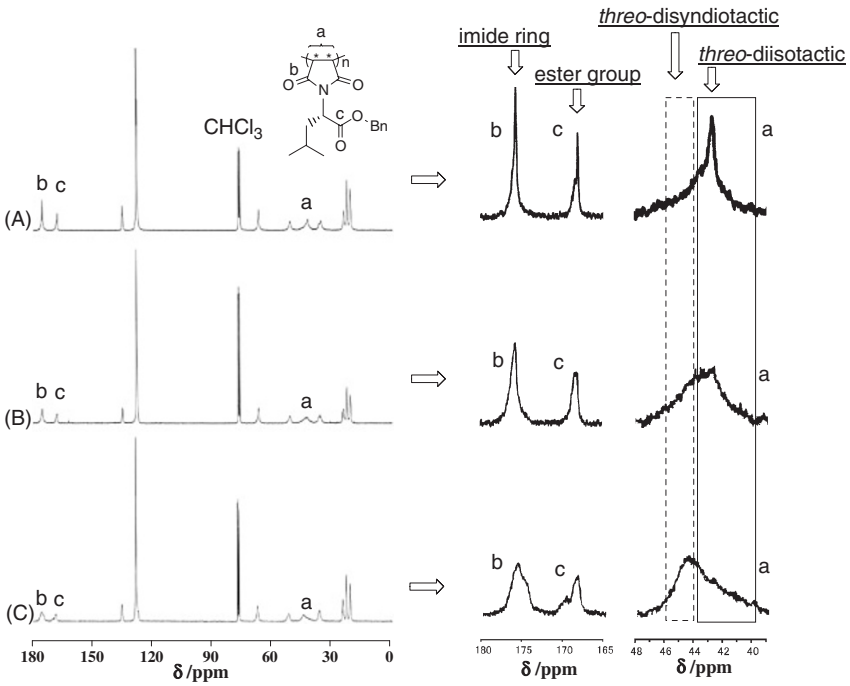

Figure 7. ^{13}C NMR spectra of poly((*S*)-BnLMI)s obtained with *n*-BuLi/Sp (1.0/1.2) in toluene ((A), $[\alpha]_{435} = -239.4^\circ$, run 6 in Table II), Et_2Zn/Sp (1.0/1.2) in toluene ((B), $[\alpha]_{435} = -109.0^\circ$, run 8 in Table II), AIBN in toluene ((C), $[\alpha]_{435} = -58.2^\circ$, run 18 in Table II).

Table III. Preparations of Poly((*S*)-RLMI)-coated Silica Gel Columns

Column[a]	Silica Gel[b]	Poly((*S*)-RLMI) (wt %)	Dispersant	Flow Rate mL/min	P_{max}[f] kg/cm^2	N[g]
1	Si-100	poly((*S*)-MLMI)[c] (5)	2-propanol	0.62	399	690
2	Si-100	poly((*S*)-MLMI)[d] (5)	2-propanol	0.61	399	312
3	Si-100	poly((*S*)-BnLMI)[e] (5)	2-propanol	0.87	399	326

[a]Column size: 150 × 2.0 mm I.D. [b]Si-100: particle size 5 μm, pore size 100 Å. [c]Poly((*S*)-MLMI): $[\alpha]_{435} = -336.0^\circ$ (run 3 in Table I). [d]Poly((*S*)-MLMI): $[\alpha]_{435} = -454.7^\circ$ (run 18 in Table I). [e]Poly((*S*)-BnLMI): $[\alpha]_{435} = -239.4^\circ$ (run 6 in Table II). [f]Highest pressure to pack CSP into column. [g]Theoretical plate number: $N = 5.54 \times (t_r/w_{1/2})$.

izations (a). Poly((*S*)-BnLMI)s obtained with anionic polymerization (a and b in Figure 7) also exhibited clear peaks belonging to the *threo*-diisotactic structures in the main chain region. The poly((*S*)-BnLMI) having higher specific rotation possesses more *threo*-diisotactic structures in the main chain. This indicates that poly((*S*)-BnLMI)s having higher specific rotation possess higher stereoregularity.

Chiral Recognition Ability of Poly((S)-RLMI)

To investigate chiral recognition abilities of poly((*S*)-MLMI) and poly((*S*)-BnLMI), CSPs for HPLC were prepared by coating poly((*S*)-MLMI) and poly((*S*)-BnLMI) on the surface of microporous silica gel. The preparation conditions of columns and theoretical plate numbers are shown in Table III. The abilities of CSPs for chiral recognition of racemates 1-31 in Chart 1 were examined with HPLC analysis using the columns prepared and the resolution results are summarized in Table IV. CSP 1, in which the poly((*S*)-MLMI) (obtained in anionic polymerization, $[\alpha]_{435} = -336.0^\circ$, run 3 in Table I) was coated on the surface of silica gel, partially resolved racemate **1** (*trans*-epoxy-1-phenyl-3-phenylpropane-3-one) listed in Chart 1 in normal phase system (*n*-hexane/2-propanol (9/1, v/v)) ($\alpha = 2.19$, $R_s = 0.68$). While CSP 2, in which the poly((*S*)-MLMI) used ($[\alpha]_{435} = -454.7^\circ$, run 18 in Table I) had higher specific rotation than that used in CSP 1, completely resolved racemate **1** in normal phase *n*-hexane/2-propanol (9/1, v/v) ($\alpha = 5.93$, $R_s = 3.89$). The typical chromatograms are shown in Figure 8. According to the data of separation factor and resolution factor, the resolution ability of CSP 2 for racemate **1** was relatively higher than CSP 1. That may be ascribed to the difference of stereoregularity of polymers, that is, the

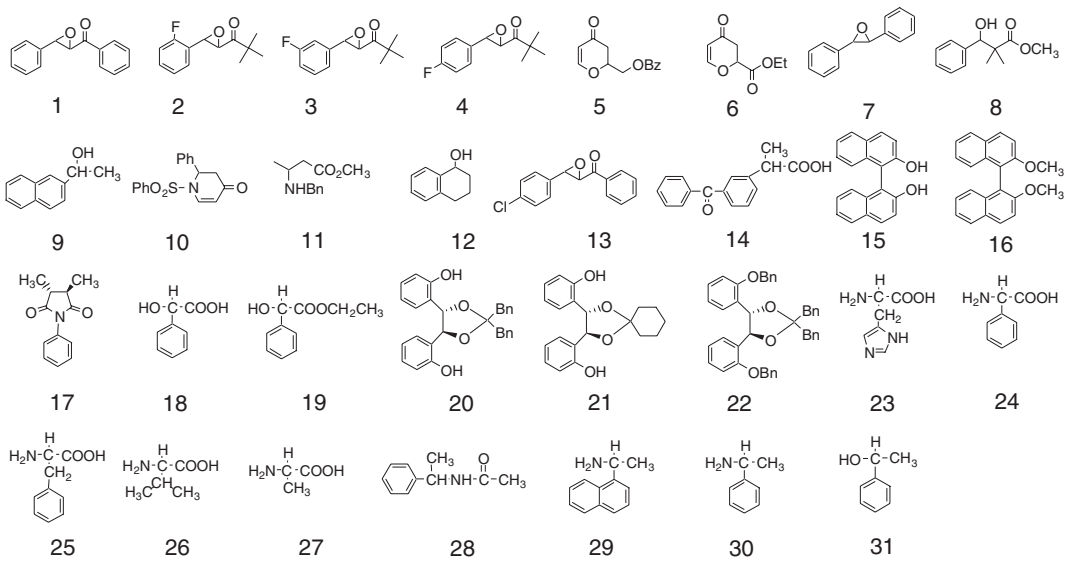

Chart 1.

Table IV. Optical Resolution Results Using Columns[a]

Run	Column	Racemate Sample[b] No.	Mobile[c] Phase (v/v)	Flow Rate mL/min	Injected Volumn μm	k_1'[d]	k_2'[d]	α[e]	R_s[f]
1	1	1	Hex/IPA (9/1)	0.50	2.5	0.21	0.46	2.19	0.68
2	2	1	Hex/IPA (9/1)	0.50	1.0	0.32	1.90	5.93	3.89

[a]See Table III. [b]See Chart 1. [c]Hex: n-hexane, IPA: 2-propanol. [d]Capacity factor of enantiomer eluting first (k_1') and second (k_2') = (retention time of enantiomer void time of column)/(retention time of 1,3,5-tri-*tert*-butylbenzene). [e]Separation factor = k_2'/k_1'. [f]Resolution factor = 2 × (distance between the peaks of more and less retained enantiomers)/(sum of bandwidth of two peaks).

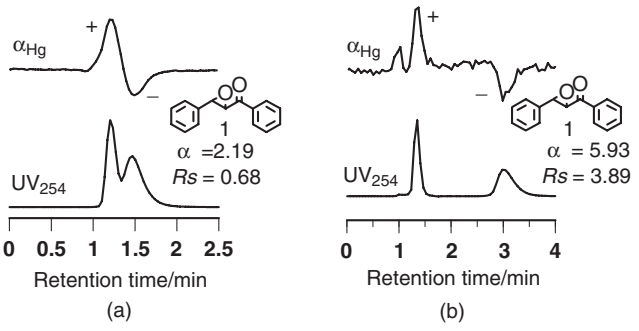

Figure 8. HPLC resolution chromatograms of racemates with (a) column 1 (Table III) listed in run 1 of Table IV, (b) column 2 (Table III) listed in run 2 of Table IV. The top chromatograms were measured by polarimetric detector (α_{Hg}) and bottom by UV detector (254 nm).

poly((*S*)-MLMI) having higher stereoregularity has higher chiral recognition ability. From the α_{Hg} chromatograms of HPLC showed in Figure 8, the (+) enantiomers of racemates were eluted at first and the (−) enantiomers were absorbed by the CSPs prepared from the poly((*S*)-MLMI) with high levorotation. The chiral discriminability of poly((*S*)-MLMI) may be ascribed not only to the interaction between the polymer and racemates but also to the higher-ordered structures of the polymer. CSP 3, in which the poly((*S*)-BnLMI) (obtained in anionic polymerization, $[\alpha]_{435} = -239.4.0^\circ$, run 6 in Table II) was coated on the surface of silica gel, resolved no racemate listed in Chart 1 in normal phase system (*n*-hexane/2-propanol (9/1, v/v)). This may be attributed to the steric exclusion of bulky benzyl group in the side chain which handicapping the approach of racemate.

CONCLUSIONS

1. Two kinds of chiral monomers (*S*)-MLMI ($[\alpha]_{435} = -35.5^\circ$) and (*S*)-BnLMI ($[\alpha]_{435} = -61.3^\circ$) were synthesized.

2. Optically active poly((*S*)-MLMI)s and poly((*S*)-BnLMI)s were obtained by asymmetric polymerizations. Poly((*S*)-MLMI) initiated by the Et_2Zn/Sp complex in toluene at −40 °C exhibited the highest negative specific rotation ($[\alpha]_{435} = -454.7^\circ$). Poly((*S*)-BnLMI) initiated by the *n*-BuLi/Sp complex in toluene showed the highest negative specific rotation ($[\alpha]_{435} = -239.4^\circ$).

3. According to the CD and GPC, optical activities of both the poly((*S*)-MLMI)s and poly((*S*)-BnLMI)s obtained with anionic polymerizations were attributed to excessive chiral centers of the main chains induced through the polymerizations in addition to the chiralities of the side groups.

4. The coated-type CSPs of poly((*S*)-MLMI) resolved racemate 1 (*trans*-epoxy-1-phenyl-3-phenylpropane-3-one) by HPLC in normal phase system such as *n*-hexane/2-propanol (9/1, v/v).

REFERENCES

1. S. E. Mallakpour, A.-R. Hajipour, A.-R. Mahdavian, and S. Khoee, *J. Polym. Sci., Part A: Polym. Chem.*, **37**, 1211 (1999).
2. F. Ciardelli, *Encycl. Polym. Sci. Eng.*, **10**, 463 (1987).
3. M. Farina, *Top. Stereochem.*, **17**, 1 (1987).
4. G. Wulff, *Angew. Chem., Int. Ed. Engl.*, **28**, 21 (1989).
5. Y. Okamoto and Y. Kaida, *J. Chromatogr. A*, **666**, 403 (1994).
6. Y. Okamoto and E. Yashima, *Angew. Chem., Int. Ed.*, **37**, 1021 (1998).
7. E. Yashima, *Anal. Sci.*, **18**, 3 (2002).
8. K. Nozaki, *J. Polym. Sci., Part A: Polym. Chem.*, **42**, 215 (2004).
9. Y. Okamoto and T. Nakano, *Chem. Rev.*, **94**, 349 (1994).
10. Y. Okamoto and T. Nakano, in "Catalytic Asymmetric Synthesis," 2nd ed, I. Ojima, Ed., Wiley-VCH, New York, 2000, Chap. 11, p757.
11. T. Oishi, K. Onimura, W. Sumida, T. Koyanagi, and H. Tsutsumi, *Polym. Bull.*, **48**, 317 (2002).
12. T. Oishi, H. Yamasaki, and M. Fujimoto, *Polym. J.*, **23**, 795 (1991).
13. T. Oishi, K. Matsusaki, and M. Fujimoto, *Polym. J.*, **24**, 1281 (1992).
14. K. Kagawa and T. Oishi, *Polym. J.*, **27**, 579 (1995).
15. K. Kagawa and T. Oishi, *Polym. J.*, **28**, 1 (1996).
16. T. Oishi, H. Nagata, and H. Tsutsumi, *Polymer*, **39**, 4135 (1998).
17. K. Onimura, H. Tsutsumi, and T. Oishi, *Macromolecules*, **31**, 5971 (1998).
18. K. Onimura, H. Tsutsumi, and T. Oishi, *Chem. Lett.*, **27**, 791 (1998).
19. T. Oishi, K. Onimura, K. Tanaka, W. Horimoto, and H. Tsutsumi, *J. Polym. Sci., Part A: Polym. Chem.*, **37**, 473 (1999).
20. H. Zhou, K. Onimura, H. Tsutsumi, and T. Oishi, *Polym. J.*, **32**, 552 (2000).
21. H. Zhou, K. Onimura, H. Tsutsumi, and T. Oishi, *Polym. J.*, **33**, 227 (2001).
22. Y. Isobe, K. Onimura, H. Tsutsumi, and T. Oishi, *Macromolecules*, **34**, 7617 (2001).
23. Y. Isobe, K. Onimura, H. Tsutsumi, and T. Oishi, *J. Polym. Sci., Part A: Polym. Chem.*, **39**, 3556 (2001).
24. T. Oishi, K. Onimura, Y. Isobe, and H. Tsutsumi, *Chem. Lett.*, **28**, 673 (1999).
25. Y. Isobe, K. Onimura, H. Tsutsumi, and T. Oishi, *Polym. J.*, **34**, 18 (2002).
26. T. Oishi, Y. Isobe, K. Onimura, and H. Tsutsumi, *Polym. J.*, **35**, 245 (2003).
27. Y. Zhang, K. Onimura, H. Tsutsumi, and T. Oishi, *Polym. J.*, **36**, 878 (2004).
28. K. Onimura, Y. Zhang, M. Yagyu, and T. Oishi, *J. Polym. Sci., Part A: Polym. Chem.*, **42**, 4682 (2004).
29. T. Oishi, Y. Zhang, T. Fukushima, and K. Onimura, *Polym. J.*, **37**, 453 (2005).
30. T. Oishi and K. Onimura, *Kobunshi Ronbunshu*, **59**, 287 (2002).
31. T. Oishi, A. Kamori, and M. Fujimoto, *J. Macromol. Sci. Pure Appl. Chem.*, **29**, 231 (1992).
32. T. Oishi, K. Kagawa, and M. Fujimoto, *Macromolecules*, **26**, 24 (1993).
33. T. Oishi and K. Onimura, *Kobunshi*, **54**, 558 (2005).
34. G. M. Coppola and H. F. Schuster, in "Asymmetric Synthesis: Construction of Chiral Molecules Using Amino Acids," John Wiley & Sons, Inc., New York, 1987.
35. G. Gao, F. Sanda, and T. Masuda, *Macromolecules*, **36**, 3932 (2003).
36. T. Oishi and M. Watanabe, JP Patent, 2005344040 2005, Kokai Tokkyo Koho, 2005.
37. H. Gao, Y. Isobe, K. Onimura, and T. Oishi, *Polym. J.*, **38**, 1288 (2006).
38. H. Gao, Y. Isobe, K. Onimura, and T. Oishi, *J. Polym. Sci., Part A: Polym. Chem.*, **45**, 3722 (2007).
39. H. Gao, Y. Isobe, K. Onimura, and T. Oishi, *Polym. J.*, **39**, 764 (2007).
40. S. E. Denmark, N. Nakajima, O. J.-C. Nicaise, A.-M. Faucher, and J. P. J. Edwards, *J. Org. Chem.*, **60**, 4884 (1995).
41. V. Ondrus and L. Fisera, *Molecules*, **2**, 49 (1997).
42. T. Oishi, K. Onimura, H. Yanagihara, and H. Tsutsumi, *J. Polym. Sci., Part A: Polym. Chem.*, **38**, 310 (2000).
43. Y. Isobe, M. Nakamura, H. Gao, K. Onimura, and T. Oishi, *Kobunshi Ronbunshu*, **63**, 484 (2006).